



Bioinspired flexible piezoresistive sensor for high-sensitivity detection of broad pressure range

Meng Wang^{1,2} · Hao Zhang² · Han Wu² · Suqian Ma² · Lei Ren² · Yunhong Liang²  · Chunbao Liu³ · Zhiwu Han²

Received: 10 July 2022 / Accepted: 21 October 2022 / Published online: 28 December 2022
© Zhejiang University Press 2022

Abstract

The human skin has the ability to sense tactile touch and a great range of pressures. Therefore, in prosthetic or robotic systems, it is necessary to prepare pressure sensors with high sensitivity in a wide measurement range to provide human-like tactile sensation. Herein, we developed a flexible piezoresistive pressure sensor that is highly sensitive in a broad pressure range by using lotus leaf micropatterned polydimethylsiloxane and multilayer superposition. By superposing four layers of micropatterned constructive substrates, the multilayer piezoresistive pressure sensor achieves a broad pressure range of 312 kPa, a high sensitivity of 2.525 kPa^{-1} , a low limit of detection (LOD) of $<12 \text{ Pa}$, and a fast response time of 45 ms. Compared with the traditional flexible pressure sensor, the pressure range of this sensor can be increased by at least an order of magnitude. The flexible piezoresistive pressure sensor also shows high robustness: after testing for at least 1000 cycles, it shows no sign of fatigue. More importantly, these sensors can be potentially applied in various human motion detection scenarios, including tiny pulse monitoring, throat vibration detection, and large under-feet pressure sensing. The proposed fabrication strategy may guide the design of other kinds of multifunctional sensors to improve the detection performance.

✉ Suqian Ma
masuqian@jlu.edu.cn

✉ Lei Ren
lei.ren@manchester.ac.uk

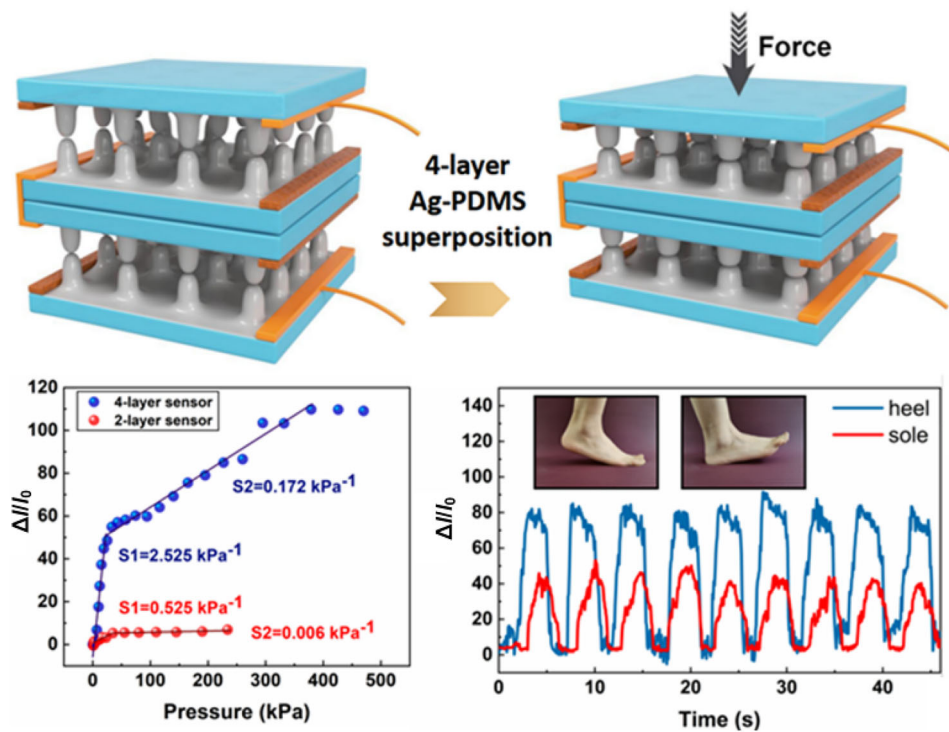
✉ Yunhong Liang
liangyunhong@jlu.edu.cn

¹ Center of Reproductive Medicine, Center of Prenatal Diagnosis, The First Hospital of Jilin University, Changchun 130021, China

² The Key Laboratory of Bionic Engineering, Ministry of Education, Jilin University, Changchun 130025, China

³ School of Mechanical and Aerospace Engineering, Jilin University, Changchun 130025, China

Graphic abstract



Keywords Bionic · Piezoresistive pressure sensor · Microstructure · Multilayer · Wide pressure range

Introduction

In the past decade, the flexible piezoresistive pressure sensor has emerged as a new type of pressure and tactile sensing method. In addition to its good response to dynamic or static stimulation and thin flexible device architecture, it has the advantages of high resolution, deformability, stretchability, low weight, and good conformal ability. With the development of robot intelligence [1, 2], electronic skin [3, 4], and wearable medical devices [5, 6], the research of flexible pressure sensing technology in medicine and industry has gradually intensified [7–13].

Among different types of sensors, piezoresistive pressure sensors have great practical application potential because of their simple structures, easy manufacturing method, high sensitivity, and low cost [14, 15]. A piezoresistive sensor consists of a flexible substrate and an electrode layer. To be able to adapt to practical applications, the desired sensor devices are expected to feature a broad pressure response range and high sensitivity.

Advanced flexible pressure sensors have been used to monitor subtle movements such as robot fingers handling delicate items [2], tactile sensing [7], noninvasive measurement of blood pressure, and large pressure motions such

as walking, running, and jumping. Different applications correspond to distinct pressure ranges: intrabody pressures [16] and palpating cardiovascular activities [17] are usually below 10 kPa; blood pressure monitoring devices [18] have high pressures of more than 10 kPa, and the plantar pressure of body weight can reach more than 100 kPa [19]. Tiny pressures are sometimes superimposed on high-pressure preloads; therefore, it is necessary to manufacture flexible pressure sensors with high sensitivity in a wide pressure range. The width of pressure range is an important feature of the sensor. When the high-pressure resolution can be preserved over a wide pressure range, it simplifies data processing and conversion. On the other hand, when the pressure range is small, the pressure applied will easily exceed the sensor measurement range, resulting in failed pressure measurement and loss of sensing function. To broaden the pressure range, Kwon et al. [20] reported a flexible and wearable pressure sensor based on three-dimensional (3D) microporous dielectric elastomer with a huge piezoelectric capacitance effect. The 3D porous elastic bridge dielectric layer could cover a wider pressure range (from 0.1 to 130 kPa) compared to those of previously reported micro/nano-structured sensing materials. However, the sensitivity was only 0.601 kPa^{-1} when the pressure was under 5 kPa,

and it decreased to 0.077 kPa^{-1} when the pressure was more than 30 kPa. Therefore, it seems a great challenge to obtain high sensitivity in a wide pressure range.

The high sensitivity of a flexible sensor allows the accurate identification of tiny pressure changes with a high signal-to-noise ratio. Meanwhile, the sensitivity of traditional piezoresistive sensors is limited by the low compressibility of the substrate. Designing microstructured substrates with higher compressibility has proved to be an effective way to increase sensitivity [21]. The commonly used method involves casting on silicon mold prepared in advance [13] or laser etching molds. Another frequently used approach is the template method. Using the above methods, substrates with micropillar arrays [12, 22], micropyramid arrays [22, 23], microdome arrays [22, 24], microcones [23], and conical frustum-like microstructures [25] can be applied in the manufacture of high-sensitivity pressure sensors. In the low pressure range, the microstructures can effectively concentrate the loads, resulting in a rapid increase in the area of contact with the loads, thus greatly improving sensitivity. However, as the pressure increases, incremental deformation and stress accumulation within the existing contact area will lead to a reduction in sensitivity, resulting in deviations from pressure. For example, Zhong et al. [26] reported a pressure sensor with ultra-high sensitivity prepared by a surface patterned nanofiber membrane (SPNM), which was obtained by simply replicating a commonly woven nylon textile. The optimal pressure sensor showed a high sensitivity of 19.4 kPa^{-1} , but the pressure range was narrow at 2.76 kPa; thus, it was not available for high pressure monitoring.

There is an abundance of reports on sensors based on polydimethylsiloxane (PDMS) films, which have different microstructures inspired by nature. Most of them have traditional sandwiched structures. Herein, we propose an effective strategy for fabricating multilayer flexible piezoresistive pressure sensors with broad pressure range and high sensitivity by using lotus leaf as a template. Compared to previous attempts, this paper adopts the method of multilayer superposition to greatly optimize the performance of the sensor and uses a simple method to ensure its superior performance. After two steps of replication, micropatterned polydimethylsiloxane (m-PDMS) was prepared for a flexible substrate, which had large-aspect-ratio and low-density papillae patterns. To make the substrate conductive, a thin silver layer was deposited on the m-PDMS surface as the sensing electrode of the piezoresistive pressure sensor. To achieve high sensitivity across a broad pressure range, four layers of m-PDMS with Ag electrode were stacked together. The fabricated multilayer flexible piezoresistive pressure sensor exhibits a high sensitivity up to 2.525 kPa^{-1} , a wide pressure range of up to 312 kPa, a fast response time of 45 ms, a low limit of detection (LOD) of $<12 \text{ Pa}$, and good stability after more than 1000 testing cycles. This sensor type has

been proven to be useful for detecting small vibrations such as wrist pulses, carotid pulse, and acoustic waves. Moreover, it was used to measure large movements like plantar pressure during walking, running, and jumping. Therefore, our flexible piezoresistive pressure sensor has great versatility and shows great development potential in future wearable devices and artificial intelligence technology.

Experimental method

Fabrication of PDMS conducting films with lotus leaf microstructure

First, fresh lotus leaves were collected in Nanhu Park of Changchun City and were cut into sizes of $4 \text{ cm} \times 2.5 \text{ cm}$ (flat large leaves without bulge were chosen). The leaves were washed 3 times with deionized water and dried at room temperature. Then, they were attached to a flat substrate by using double-faced adhesive tapes.

Second, the m-PDMS flexible film was fabricated. Epoxy base and curing agent were mixed (base:curing agent=3:1 by weight) by mechanical stirring at least for 10 min. After degassing, the mixture was poured onto the surface of the lotus leaf, degassed again and cured 20 h at room temperature. The lotus leaf was stripped from the surface, and epoxy mold with reverse structure was prepared. The PDMS solution (Dow Corning Sylgard 184; prepolymer base:curing agent=10:1 by weight) was prepared by mechanical stirring for 15 min, degassed again and poured onto the negative epoxy mold. Degassing was performed once more to facilitate PDMS infiltration and heating followed at $80 \text{ }^\circ\text{C}$ for 2 h, and then, the m-PDMS thin film was easily peeled off from the epoxy mold. Epoxy mold is a very strong thermosetting material with corrosion resistance and no deformation. Therefore, the epoxy mold can be used for extended periods, and the resulting PDMS base layer microstructure morphology is stable.

Third, the flexible electrode was prepared by sputter-coating (108 auto Cressington sputter coater) metal Ag (thickness=70 nm) onto the m-PDMS. The thickness of Ag film was controlled through changing the spray time (90 s) and the spray current (30 mA). Finally, the m-PDMS conductive film formed by a lotus leaf was obtained.

Fabrication of flexible E-skin

The flexible pressure sensor of this work was composed of four layers of m-PDMS conductive films. We placed the rough surfaces face-to-face and stuck the flat surfaces as shown in Fig. 1a. Copper wires that were soldered onto the copper tape were adhered to the border of Ag films (Fig. 2c). The copper tape did not touch any other film surface due

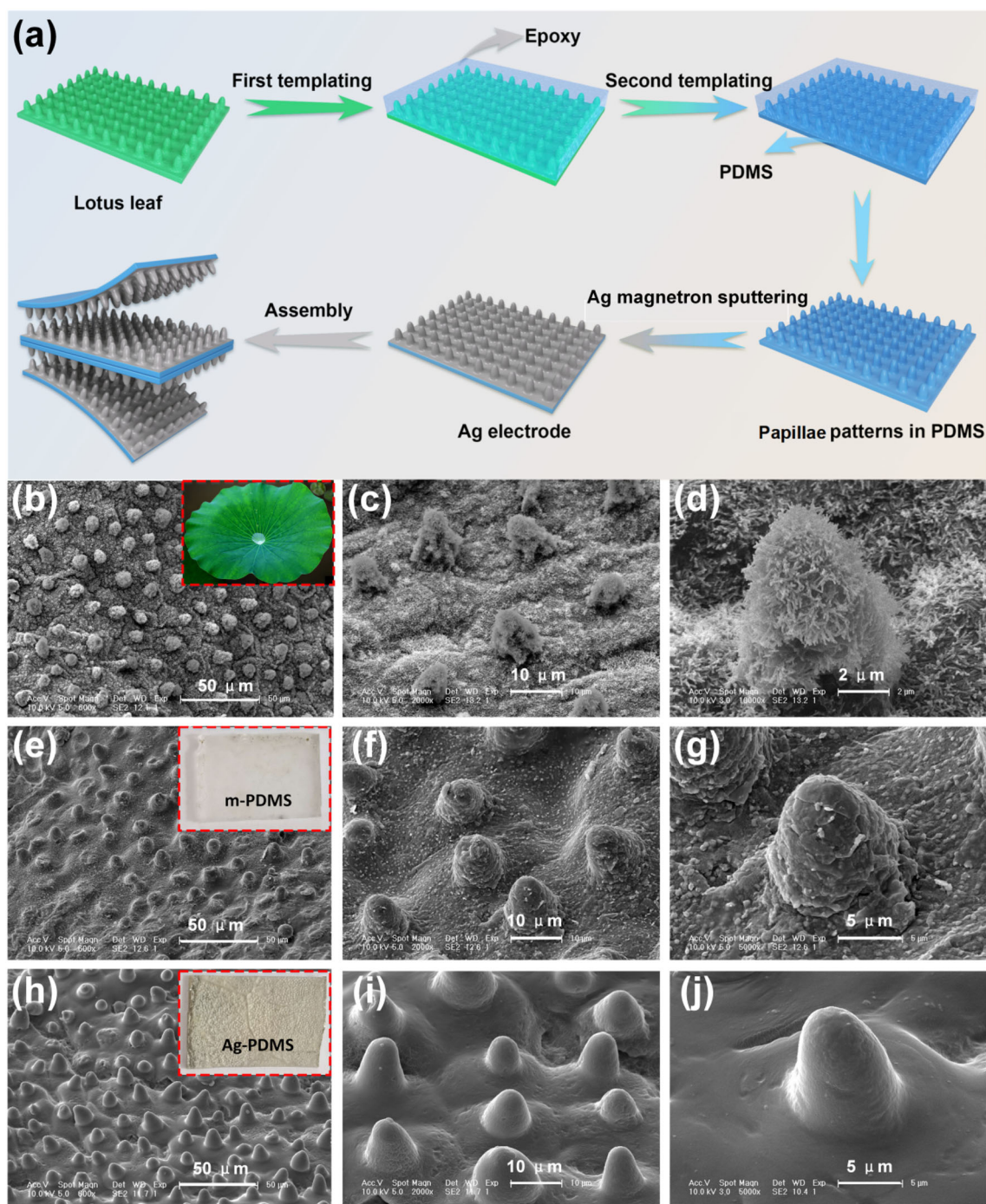


Fig. 1 Preparation process of flexible piezoresistive pressure sensor and the scanning electron microscope (SEM) images of the microstructure. **a** Schematic illustration of the fabrication process of a pressure sensor device. **b–d** 45° tilt view SEM images of a lotus leaf. Scale bar: 50 μm ,

10 μm , 2 μm . **e–g** 45° tilt view SEM images of m-PDMS. Scale bar: 50 μm , 10 μm , 5 μm . **h–j** 45° tilt view SEM images of a patterned Ag-PDMS. Scale bar: 50 μm , 10 μm , 5 μm . PDMS: polydimethylsiloxane

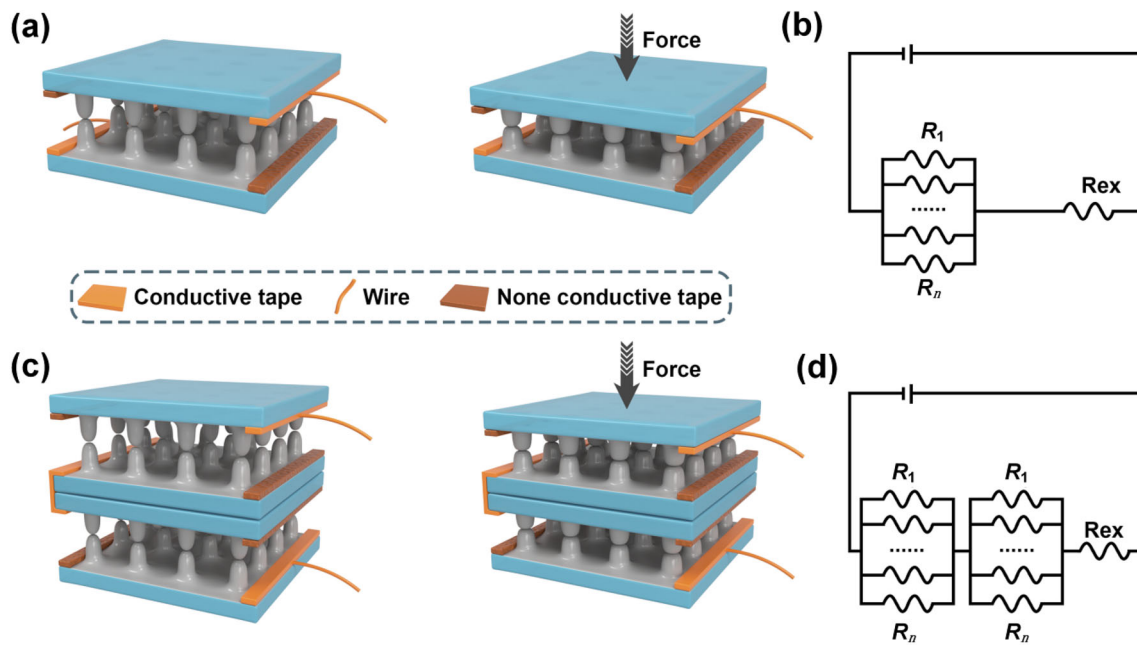


Fig. 2 Characterization of the flexible piezoresistive pressure sensor with two layers and four layers, respectively. **a** Schematic diagram of the working mechanism of the two-layer sensor with pressure applied. With rising pressure, the contact area between the electrode layers enlarges. **b** The proposed equivalent circuit diagram of the two-layer sensor. Each

papilla is considered as a variable resistor (R_n), and its resistance value is dependent on the contact area of the papillae with the opposite side contact point. **c** Schematic diagram of the working mechanism of the four-layer sensor with pressure applied. **d** The proposed equivalent circuit diagram of the four-layer sensor

to covering the non-conductive tape (Fig. 2c). In the end, the four edges of the sensor were covered by polyethylene terephthalate (PET), and the flexible pressure sensor with high performance was produced.

Structure characterization

Surface characterizations and energy spectrum were obtained by a scanning electron microscope (SEM, XL-30 ESEM FEG, FEI COMPANY, Hillsboro, USA). The height of the surface microbumps was obtained by confocal microscopy (06003842, Olympus Corporation, Japan).

Testing of pressure sensing performance

All testing experiments of the sensors were carried out using a universal testing machine (WDW-05) controlled by a micro-computer. The resistance of the sample was measured by a digital precision multimeter (Keysight, 34465A) (Fig. S4 in Supplementary Information). To determine the low detection limit, a small super light clay (0.476 g) was placed onto a pressure sensor device (4 cm² in area). The test on a human body was conducted on a healthy volunteer, Han Wu, with his consent.

Results and discussion

Design principle and fabrication of piezoresistive pressure sensor

We fabricated a multilayer structured flexible piezoresistive pressure sensor by using lotus leaf as a template. Figure 1a and Fig. S1 (Supplementary Information), respectively, present the manufacturing process and physical image of the flexible piezoresistive pressure sensor. The substrate with microstructure was obtained by using the template method. After the microstructure of lotus leaf was reproduced, an Ag film was sputtered on the m-PDMS substrate. For better replication quality, PDMS (base:curing agent=10:1 by weight) was utilized, as it is suitable for replicating nanoscale patterns. The greater the compressibility of material used, the broader pressure range and the greater sensitivity of the fabricated sensor [27]. To improve the pressure range and sensitivity of pressure sensors, dielectric layers with low Young's modulus are often used. Nevertheless, a softer base layer usually exhibits higher viscosity, and PDMS with unstructured surface results in an increase in viscosity, both of them leading to lower response speeds. Therefore, soft and highly sticky base layers should be avoided. In this work, m-PDMS (base:curing agent=10:1 by weight) allowed for easier deformation and faster response speed at the same time.

The introduction of lotus leaf microstructure can improve the sensitivity of the sensor and reduce the manufacturing cost. Figures 1b–1d present the SEM images of the surface structure on the lotus leaf, indicating that the surface of lotus leaf is composed of randomly distributed nanoscale papillae. A 3D confocal image can be seen in Fig. S2 (Supplementary Information), which shows that the height of the papillae on the Ag-PDMS film is from 7 to 16 μm , the base width of the papillae is from 5 to 12 μm , and the average distance between papillae is about 20 μm . The microstructures on the surface of lotus leaf have a higher aspect ratio to deform, and there is more room to compress. Moreover, the lower the density of the microstructure, the “softer” the dielectric layer, and thus the pressure range and the sensitivity can be improved. Microstructures are more compressible with smaller sizes and when they are more dispersed [28]. The papillae structures have an uneven stress distribution where the stress is concentrated at the top. For a given applied stress, microstructures have greater local stress concentration than non-structured surfaces, which can lead to greater changes in the contact area. Figures 1e–1g show the SEM images of PDMS with microstructures, where the papillary microstructure has been copied onto the PDMS membrane. Figures 1h–1j illustrate the presence of papillary structure on an Ag-PDMS film, demonstrating that the stacked metal Ag has entirely covered the surface of m-PDMS (Fig. S3 in Supplementary Information). By adjusting the sputtering current and the sputtering time of metal Ag, the thickness of Ag electrode can be easily controlled. When studying the thickness of the conductive silver layer, the thinner (40 nm) ones have low conductivity and low resistance change, while the thicker (120 nm) ones have stable resistance but low response impedance. Thus, the silver layer with the thickness of 70 nm exhibits stable resistance and high response impedance (Fig. S4 and Table S1 in Supplementary Information); therefore, it was chosen in this study.

The design concept of this sensor includes four layers of Ag-PDMS stacked together to increase the sensitivity while also extending the pressure range. For comparison, the working mechanism of the traditional two-layer sensor is demonstrated in Figs. 2a and 2b. When a constant voltage of 1 V is applied to the sensor, the current flows through the papillae tip to the opposite side contact point, and each tip is similar to the resistor in a parallel circuit. When external pressure is applied to the sensor, it will cause deformation of the papillary structure, leading to an increased contact area between the papillary tip and the opposite side contact point, and the conductive path increases accordingly. This leads to a drop in the resistance of the device, which results in an increase in the current. Due to the elastic properties of PDMS, the papillae structure will return to its initial state when the pressure is released. Thus, the conductive path decreases and

the resistance increases. To build a superior flexible piezoresistive pressure sensor device, four layers of Ag-PDMS films were stacked together face to face (Fig. 2c). In the novel four-layer structure, four electrode layers were superimposed face to face, equivalent to two resistor devices in series (Fig. 2d); so, the initial resistance multiplied compared with a two-layer sensor. Relative to a single resistance device, the four-layer structure has more contact points under the same pressure, and the relative resistance changes will be greater. The four-layer structure has four layers of m-PDMS and thus greater compressibility, and the sensitivity of the corresponding sensor will be higher. The contact area of the two-layer sensor will be saturated at a small pressure, and it reaches the upper limit of the pressure measurement range. However, in the four-layer sensor, which has more papillae structures and greater compressibility, more pressure is needed to reach the saturation of contact area, so the pressure range is broader. Therefore, a multilayer superposition of papillae microstructures and the flexible property of PDMS should render the sensor excellent sensing performance.

Sensing performance under pressure

In order to investigate the effect of the four-layer m-PDMS electrode superposition on the sensing performance, a traditional two-layer m-PDMS electrode sensor was fabricated for comparison. To quantitatively evaluate the sensing performance of the sensor, the change of current with pressure was monitored by a digital source meter equipped with a compression testing machine, as shown in Fig. S5 (Supplementary Information). At a voltage of 1 V, the real-time current was recorded while increasing the applied vertical pressure. The curve of loading force versus time and the curve of integrated current versus time are demonstrated in Fig. S6 (Supplementary Information). The results indicate that as the pressure on the device increases, so does the measured current. According to the results shown in Fig. S6 (Supplementary Information), the relative current change $\Delta I/I_0$ at different load pressures is calculated. Figure 3a shows that the relative current change increases with increasing load pressure. The sensitivity of the pressure sensor can be obtained by calculating the data in Fig. 3a, which is determined according to the following formula:

$$S = (\Delta I/I_0)/\Delta P, \quad (1)$$

where I_0 represents the initial current without pressure loaded, ΔI represents the difference between the initial current and instantaneous current under regular pressure, and ΔP is the change in the loaded pressure [29]. As demonstrated in Fig. 3a, the variation in current curve with the change in applied pressure is obtained. For the four-layer sensor, the sensitivity of the device reaches 2.525 kPa^{-1} when

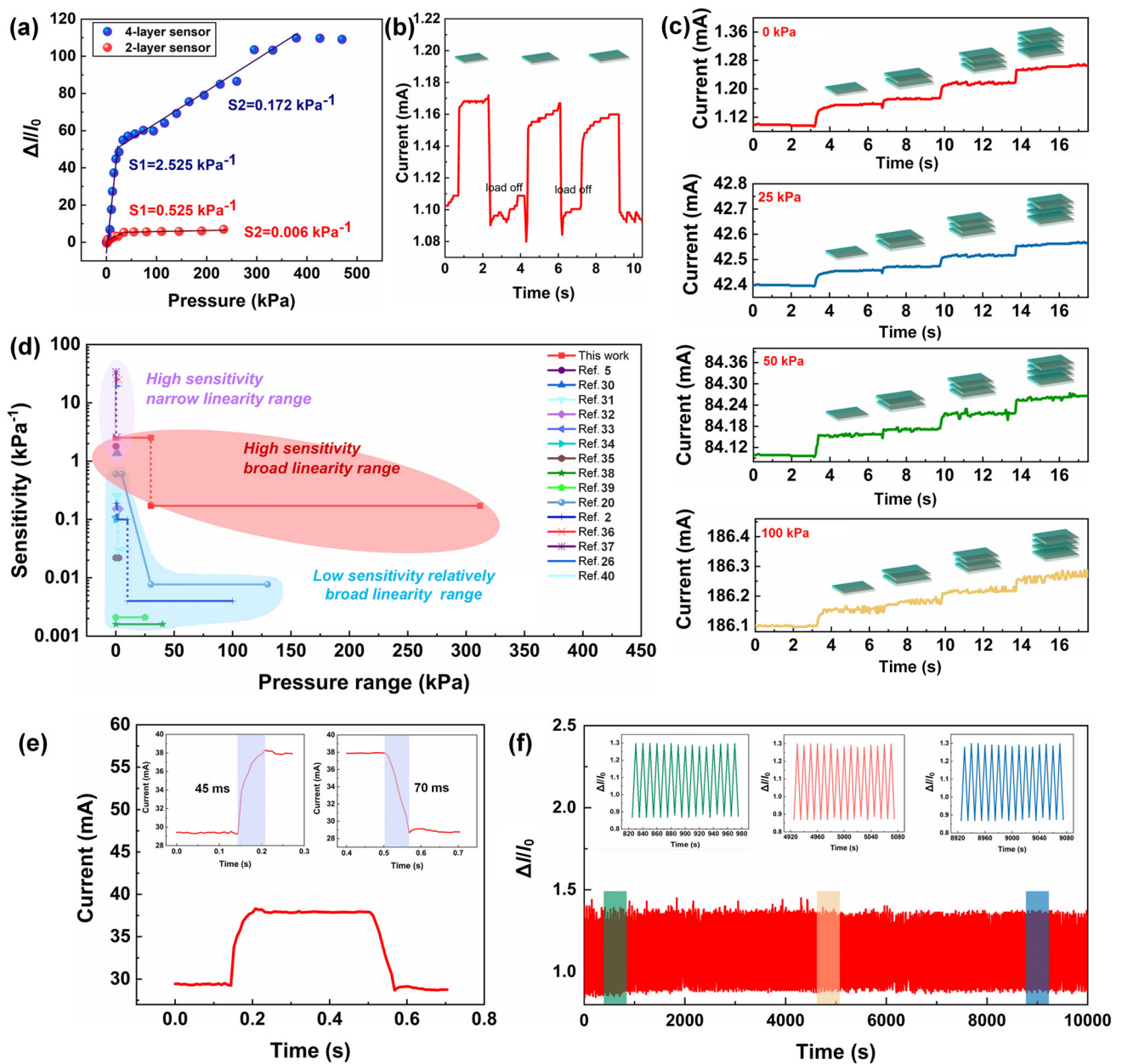


Fig. 3 Properties of the piezoresistive pressure sensors. **a** Sensitivity of the four-layer (blue sphere) and two-layer sensor (red sphere). **b** Current-time curve recorded on the sensor device when the weighting super light clay repeating the loading and unloading processes. **c** Detection of super light clay stacked onto the sensor device that has been preloaded with pressures of 0, 25, 50, and 100 kPa. **d** The sensitivity

of our pressure sensor compared with other flexible pressure sensors. **e** The response time and recovery time of the pressure sensor under 25 g weight of loading pressure and unloading pressure. **f** The durability of pressure sensor was tested by repeated loading and unloading operations (the total duration was 10,000 s, 1000 circles) with a pressure of $\approx 6 \text{ kPa}$

of the pressure is less than 30 kPa. Meanwhile, in the pressure region of 30–312 kPa, the sensitivity of the device is 0.172 kPa^{-1} ; by contrast, the two-layer sensor shows sensitivities of 0.525 and 0.006 kPa^{-1} in the pressure regions of 0–34 kPa and higher than 34 kPa, respectively, which are less than those for the four-layer sensor. It follows that the sensitivity of a four-layer sensor is 5 times larger than that

of the traditional two-layer sensor, and the pressure range of the four-layer sensor can increase by an order of magnitude compared to that of the two-layer sensor. In the four-layer structure, four m-PDMS electrode layers are superimposed. The pressure measurement range of the four-layer structure reaches 312 kPa, and the sensitivity is also high enough to meet the pressure measurement of various parts of the human

body and various movement modes; hence, the sensing performance of the four-layer sensor is sufficient. The pressure range of a six-layer structured sensor will be wider, but the thickness of the device will also increase accordingly, which will affect the wearing comfort. Therefore, we chose a four-layer structure sensor.

Compared with the two-layer sensor, the four-layer sensor can saturate the contact area under greater pressure, so it has a much broader pressure range. At the same time, the four-layer sensor's contact area is greater under the same pressure, and both the current increase and the sensitivity are higher. To measure the LOD of the sensor, a 2 cm × 2 cm piece of super light clay (0.476 g, 11.66 Pa) was loaded evenly on the device surface, as shown in Fig. S7 (Supplementary Information), and the LOD of the sensor was 11.66 Pa. Figure 3b shows that after repeating the loading and unloading processes of the clay (0.476 g, 11.66 Pa) several times (Fig. S7 in Supplementary Information), it was revealed that the sensor is quite sensitive to a tiny pressure, and the current change is stable. Additionally, the tiny pressure (four pieces of super light clay in similar sizes were stacked on the sensor surface) could be successfully recognized even when the low pressure (0 and 25 kPa) or high pressure (50 and 100 kPa) had been preloaded onto the sensor (Fig. S8 in Supplementary Information), as shown in Fig. 3c. The current also increased with the loading pressure.

The comparisons of sensitivity and detecting range with other reported flexible pressure sensors are summarized in Fig. 3d and Table S2 (Supplementary Information) [2, 5, 20, 26, 30–40]. Sensors with high sensitivity ($1.35\text{--}34\text{ kPa}^{-1}$) usually have narrow pressure ranges below 3 kPa. Meanwhile, sensors with broad pressure ranges (0–130 kPa) usually have low sensitivities of up to 0.26 kPa^{-1} . For example, Boutry et al. [2] reported a biomimetic soft electronic skin with pyramid microstructures, which were arranged along phyllotaxis spirals as inspired by nature, and had a pressure range of 0–100 kPa and a sensitivity of 0.19 kPa^{-1} . Kwon et al. [20] developed a wearable pressure sensor based on the giant piezocapacitive effect of a 3D microporous dielectric elastomer, which showed a pressure range of 0–130 kPa and a sensitivity of 0.601 kPa^{-1} . In this work, the sensor not only featured a much broader pressure range of 0–312 kPa, which is 2 or 3 times larger than that of sensors described above, it also featured high sensitivity of 2.525 kPa^{-1} , which is almost an order of magnitude higher than those in previously reported works. Such a large pressure range can satisfy the pressure range occurring in all parts of the human body and various sports, especially for monitoring the pressure of lower limbs' movements, which can be used for the sensing of lower limb prosthetics to realize their intelligent application. To study the response time of our resistance pressure sensor, we placed a 25 g weight on the surface of the sensor. As exhibited in Fig. 3e, the

current of sensor rose rapidly after a rapid response time of 45 ms, which is equivalent to the response time of the human skin (30–50 ms) [41]. After releasing the pressure, the sensor current decreased rapidly with the short recovery component within about 70 ms and then decayed to its initial value (Fig. 3e). The difference in loading response times may be attributed to the unloading speed that was slower than the loading speed.

The stability of the four-layer flexible pressure sensor was tested through repeated loading and unloading of 6 kPa pressure 1000 times. Using the computer, the universal testing machine was programmed to circularly apply 6 kPa pressure on the pressure sensor surface 1000 times, and the current was monitored throughout the pressure changes. As shown in Fig. 3f, the reliability and the repeatability of the sensor were proven: There was little change of $\Delta I/I_0$. Figure 3f also shows the signal under three phases of the repeated tests with very similar waveforms, and that no fatigue occurred during the 1000 loading and unloading cycles. Therefore, the piezoresistive pressure sensor in this work exhibits excellent performance regarding high sensitivity, broad pressure range, low LOD, and good stability and reliability. Generally, for most piezoresistive pressure sensors, high sensitivity is obtained in the low pressure ranges [26, 36, 37]. However, the sensitivity of these sensors usually becomes very low in the high pressure range, which greatly limits their practical application in motion monitoring [26, 36, 37]. In this work, under the pressure of 30 kPa, the sensitivity was retained at about 2.525 kPa^{-1} , and the pressure-detecting range reached 312 kPa, which is much wider than those in previously published works [26]. Moreover, the response time of the sensor in this study was 45 ms, which can meet the requirements for most of the practical pressure measurements. Owing to these characteristics, the proposed pressure sensor has great potential for the quantitative detection of various human activities when used as E-skins, lower limb prosthetic sensing equipment, or health monitoring devices.

Physiological signal detection

Piezoresistive pressure sensors have great flexibility, high sensitivity, and wide detection range, which can be used to monitor a variety of physiological signals and physical motions. Our flexible device can be gently and conveniently attached onto the neck and wrist with tapes to measure pulse vibrations, as exhibited in Fig. 4a. Pulse wave is an important physiological phenomenon that can be detected along the arterial system and contains a large number of reliable signals. From the pulse intensity, frequency, and reflection, medical experts can gather information about blood pressure (BP), velocity, viscosity, blood flow resistance, and vascular wall status, which can aid diagnosis and prevention of cardiovascular disease [42]. Figure 4b exhibits the real-time pulse

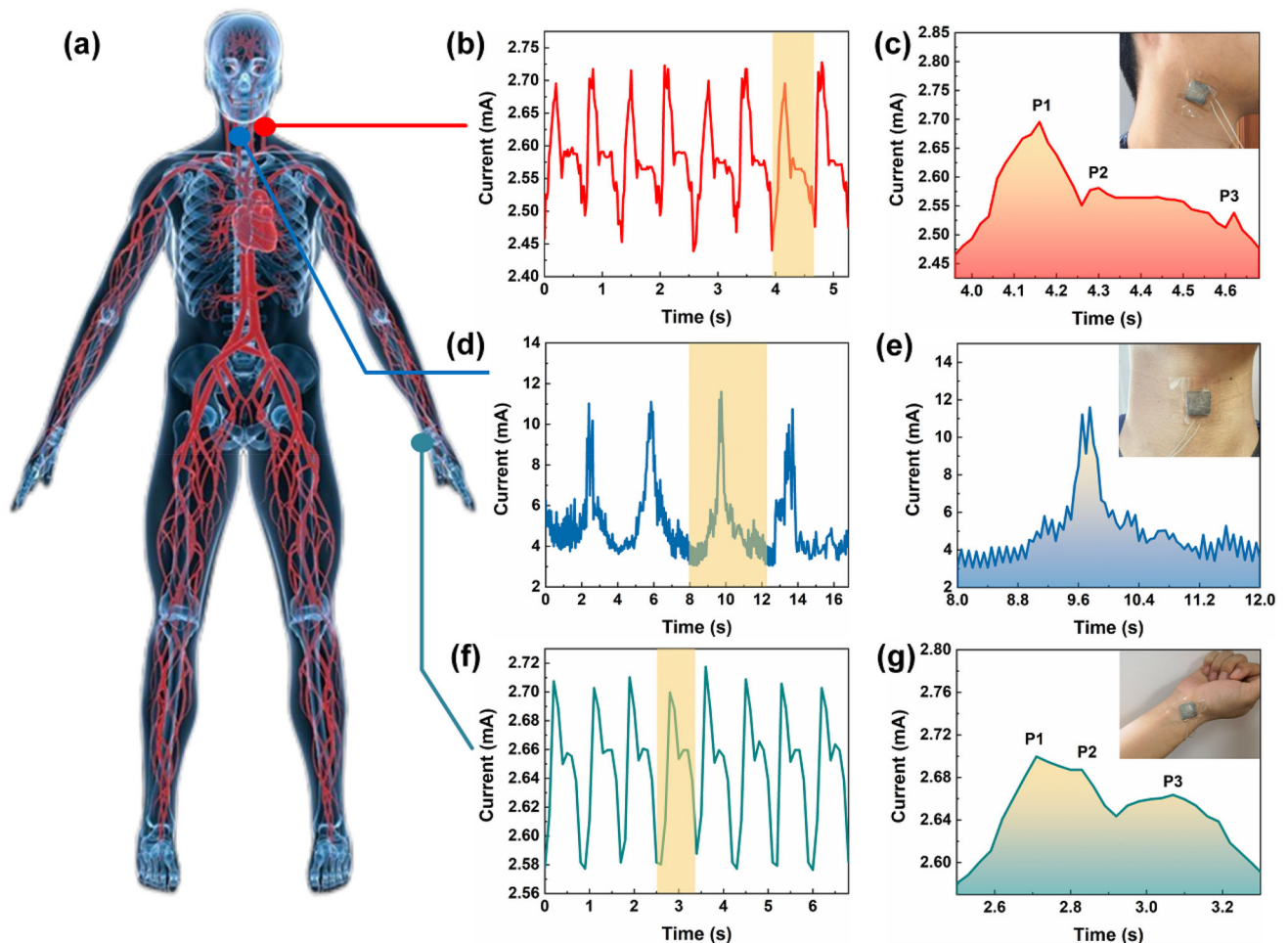


Fig. 4 Applications of the piezoresistive pressure sensor under a voltage of 1 V. **a** Photograph of the location pressure sensor attached to the neck and wrist with tapes to measure pulse vibrations. **b, c** Real-time current

variation of carotid artery pulse monitoring. **d, e** Real-time current variation of vocal cord vibration monitoring for the utterance of “Hello.” **f, g** Real-time current variation of radial artery pulse monitoring

monitoring of the volunteer’s carotid artery, and there are approximately 8 peaks in 6 s (80 pulses/min). In the magnified diagram of a single pulse cycle (Fig. 4c), the pulse wave characteristics of percussion wave (P1), tidal wave (P2), and dicrotic wave (P3) can be distinguished clearly. Figure 4f demonstrates the real-time pulse monitoring of the radial artery in a volunteer using our piezoresistive pressure sensor. Figure 4g can clearly distinguish between the pulse wave characteristics of percussion wave (P1), tidal wave (P2), and dicrotic wave (P3). Besides the pulse signals, the vibration of the vocal cord can be detected by the sensor. Figure 4d exhibits the real-time current output of the volunteer saying “Hello” in English, which reveals that the pressure sensor can produce highly repeatable, strong current signals and identifiable peaks. By amplifying the “Hello” peak signal, the waveform of the phrase has changed slightly (Fig. 4e). This observation indicates that our pressure sensor has the ability of “identifying” and “speaking.” The above experiments

reveal the ability of the piezoresistive pressure sensor of this paper to detect tiny signals.

The experiment showed that the sensor is stable and sensitive in a broad detection range; therefore, it has a good ability to detect high pressures. Here, the sensor was applied to monitor the gait of a human volunteer. The average plantar pressure of an adult male (weighing 75 kg and wearing shoes of U.S. size 8.5) in static standing state is about 35 kPa [43]. Our piezoresistive pressure sensor can work well under the continuous pressure of the soles. We first installed piezoresistive pressure sensors on the sole of foot and the heel of the foot (shown in Figs. 5a and 5b). The two sensors were connected to two digital multimeters to simultaneously detect current changes caused by foot pressure during slow walking. Figures 5a and 5b present the real-time signal waves with different relative current changes of the sole and heel. The blue curve indicates the change in relative current generated by the heel, which is larger than the red

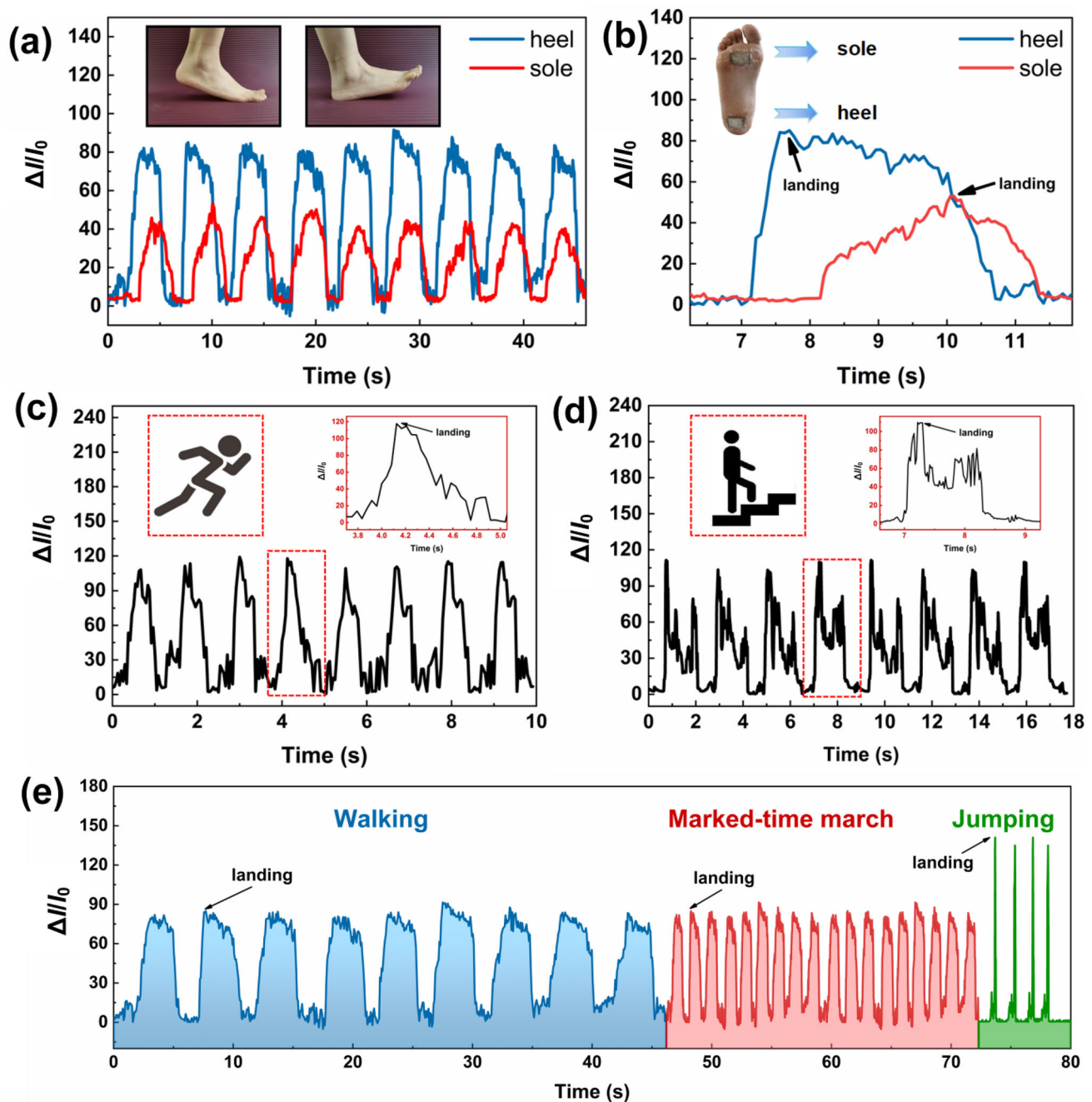


Fig. 5 Human gait monitoring of the sensor. **a** Current change signal of the sole and heel pressure detected during walking. **b** A single period of the current change of the sole and heel pressure detected during walking. **c** Current change signal of the heel pressure detected during

running. **d** Current change signal of the heel pressure detected during climbing the stairs. **e** Current change signal of heel pressure detected during walking, marked-time march, and jumping

curve showing the relative current change generated by the sole. This is because the heel usually bears more pressure than the sole while walking. Figure 5c shows the current signal change of the heel pressure while running on the treadmill at the speed of 6 km/h; the peaks of landing can be clearly observed. Figure 5d illustrates the current signal

change of the heel pressure while climbing the stairs; the curve shows the fluctuations of landing. Figure 5e exhibits the current signal change with specific amplitudes and frequencies. Slow walking corresponds to a low frequency that is reflected in a stable periodic waveform. Meanwhile, the fast marked-time march results in an increased frequency

and weak intensity. Jumping yields sharp peaks of landing and has a volatility curve of taking off. Since our sensors have good sensitivity at high pressure, the different motion modes can be easily differentiated from the waveforms.

Conclusions

In this work, a flexible, sensitive and large pressure range piezoresistive pressure sensor was designed and prepared using a multilayer superposition method with papillae microstructural electrode layers. The papillae microstructures obtained through the template method were used to improve the sensitivity, and the purpose of multilayer superposition strategy was to get broad pressure range and high sensitivity. In the experiment, the flexible pressure sensor showed a sensitivity of 2.525 and 0.172 kPa⁻¹ in a pressure range of less than 30 and 30–312 kPa, respectively. Moreover, it had a fast response time (within 45 ms), low detection limit (less than 12 Pa), and good reproducibility over 1000 cycles. It showed a pressure measurement over a very broad range of 0–312 kPa. These piezoresistive pressure sensors could recognize vocal band vibration and measure human pulses and also demonstrated the ability to monitor the plantar pressure under multiple movement patterns owing to the broad pressure range. In addition, they exhibited high sensitivity even under a large preload. These remarkable features indicate that the proposed sensor has great application potential in the field of wearable electronics, motion monitoring, health monitoring, and human interface technologies, especially in applications with high pressure ranges.

Supplementary Information The online version contains supplementary material available at <https://doi.org/10.1007/s42242-022-00220-4>.

Acknowledgements This work was supported by the Project of National Key Research and Development Program of China (No. 2018YFC2001300), the National Natural Science Foundation of China (Nos. 52175271, 51822504, 52021003, 52105299, 51905207, and 91948302), Science and Technology Development Plan Project of Jilin Province (No. 20210508057RQ), Program for Jinlin University Science and Technology Innovative Research Team (No. 2017TD-04), and Scientific Research Project of Education Department of Jilin Province (No. JJKH20211084KJ).

Author contributions SQM was involved in conceptualization; MW contributed to funding acquisition; MW, HZ, YHL, and LR were involved in investigation; HW contributed to project administration; YHL was involved in supervision; MW, HZ, SQM, and YHL contributed to visualization; CBL, MW, and ZWH were involved in writing—original draft; MW and SQM contributed to writing—review and editing.

Declarations

Conflict of interest The authors declare that they have no conflict of interest.

Ethical approval Additional informed consent was obtained from all participants for which identifying information is included in this article. All procedures followed were in accordance with the ethical standards of the responsible committee on human experimentation (institutional and national) and with the Helsinki Declaration of 1975, as revised in 2008 (5). Informed consent was obtained from all patients for being included in the study.

References

- Zhan Z, Lin R, Tran VT et al (2017) Paper/carbon nanotube-based wearable pressure sensor for physiological signal acquisition and soft robotic skin. *ACS Appl Mater Interfaces* 9(43):37921–37928. <https://doi.org/10.1021/acsami.7b10820>
- Boutry CM, Negre M, Jorda M et al (2018) A hierarchically patterned, bioinspired skin able to detect the direction of applied pressure for robotics. *Sci Robot* 3(24):eaau6914. <https://doi.org/10.1126/scirobotics.aau6914>
- Bermúdez GSC, Fuchs H, Bischoff L et al (2018) Electronic-skin compasses for geomagnetic field-driven artificial magnetoreception and interactive electronics. *Nat Electron* 1:589–595. <https://doi.org/10.1038/s41928-018-0161-6>
- Wang C, Wang DH, Yu Z et al (2013) User-interactive electronic skin for instantaneous pressure visualization. *Nat Mater* 12:899–904. <https://doi.org/10.1038/nmat3711>
- Wang XW, Gu Y, Xiong ZP et al (2014) Silk-molded flexible, ultrasensitive, and highly stable electronic skin for monitoring human physiological signals. *Adv Mater* 26(9):1336–1342. <https://doi.org/10.1002/adma.201304248>
- Qi K, He JX, Wang HB et al (2017) A highly stretchable nanofiber-based electronicskin with pressure-, strain-, and flexion-sensitive properties for health and motion monitoring. *ACS Appl Mater Interfaces* 9(49):42951–42960. <https://doi.org/10.1021/acsami.7b07935>
- Mannsfield SCB, Tee BCK, Stoltenberg RM et al (2010) Highly sensitive flexible pressure sensors with microstructured rubber dielectric layers. *Nat Mater* 9:859–864. <https://doi.org/10.1038/nmat2834>
- Hammock ML, Chortos A, Tee BCK et al (2013) 25th anniversary article: the evolution of electronic skin (e-skin): a brief history, design considerations, and recent progress. *Adv Mater* 25(42):5997–6038. <https://doi.org/10.1002/adma.201302240>
- Wang Y, Wang L, Yang T et al (2014) Wearable and highly sensitive graphene strain sensors for human motion monitoring. *Adv Funct Mater* 24(29):4666–4670. <https://doi.org/10.1002/adfm.201400379>
- Roh E, Hwang BU, Kim D et al (2015) Stretchable, transparent, ultrasensitive, and patchable strain sensor for human–machine interfaces comprising a nanohybrid of carbon nanotubes and conductive elastomers. *ACS Nano* 9(6):6252–6261. <https://doi.org/10.1021/acs.nano.5b01613>
- Zhang Y, Hu Y, Zhu P et al (2017) A flexible and highly sensitive pressure sensor based on microdome-patterned PDMS forming with assistance of colloid self-assembly and replica technique for wearable electronics. *ACS Appl Mater Interfaces* 9(41):35968–35976. <https://doi.org/10.1021/acsami.7b09617>
- Park H, Jeong YR, Yun J et al (2015) Stretchable array of highly sensitive pressure sensors consisting of polyaniline nanofibers

- and Au-coated polydimethylsiloxane micropillars. *ACS Nano* 9(10):9974–9985. <https://doi.org/10.1021/acsnano.5b03510>
13. Zhu B, Niu Z, Wang H et al (2014) Microstructured graphene arrays for highly sensitive flexible tactile sensors. *Small* 10(18):3625–3631. <https://doi.org/10.1002/smll.201401207>
 14. Tsai Y, Wang C, Chang T et al (2019) Multilayered Ag NPs-PEDOT-paper composite device for human-machine interfacing. *ACS Appl Mater Interfaces* 11(10):10380–10388. <https://doi.org/10.1021/acscami.8b21390>
 15. Shuai X, Zhu P, Zeng W et al (2017) Highly sensitive flexible pressure sensor based on silver nanowires-embedded polydimethylsiloxane electrode with microarray structure. *ACS Appl Mater Interfaces* 9(31):26314–26324. <https://doi.org/10.1021/acscami.7b05753>
 16. Kim JH, Caprioli J (2018) Intraocular pressure fluctuation: is it important? *J Ophthalmic Vis Res* 13:170
 17. Choong CL, Shim MB, Lee BS et al (2014) Highly stretchable resistive pressure sensors using a conductive elastomeric composite on a micropillar array. *Adv Mater* 26(21):3451–3458. <https://doi.org/10.1002/adma.201305182>
 18. Li Z, Wang ZL (2011) Air/liquid-pressure and heartbeat-driven flexible fiber nanogenerators as a micro/nano-power source or diagnostic sensor. *Adv Mater* 23(1):84–89. <https://doi.org/10.1002/adma.201003161>
 19. Lou C, Wang S, Liang T et al (2017) A graphene-based flexible pressure sensor with applications to plantar pressure measurement and gait analysis. *Materials* 10(9):1068. <https://doi.org/10.3390/ma10091068>
 20. Kwon D, Lee TI, Shim J et al (2016) Highly sensitive, flexible, and wearable pressure sensor based on a giant piezocapacitive effect of three-dimensional microporous elastomeric dielectric layer. *ACS Appl Mater Interfaces* 8(26):16922–16931. <https://doi.org/10.1021/acscami.6b04225>
 21. Ruth SRA, Beker L, Tran H et al (2019) Rational design of capacitive pressure sensors based on pyramidal microstructures for specialized monitoring of biosignals. *Adv Funct Mater* 30(29):1903100. <https://doi.org/10.1002/adfm.201903100>
 22. Park J, Kim J, Hong J et al (2018) Tailoring force sensitivity and selectivity by microstructure engineering of multidirectional electronic skins. *NPG Asia Mater* 10:163–176. <https://doi.org/10.1038/s41427-018-0031-8>
 23. Santos A, Pinela N, Alves P et al (2018) Piezoresistive e-skin sensors produced with laser engraved molds. *Adv Electron Mater* 4(9):1800182. <https://doi.org/10.1002/aelm.201800182>
 24. Chen M, Li K, Cheng G et al (2019) Touchpoint-tailored ultrasensitive piezoresistive pressure sensors with a broad dynamic response range and low detection limit. *ACS Appl Mater Interfaces* 11(2):2551–2558. <https://doi.org/10.1021/acscami.8b20284>
 25. Shi J, Liu W, Dai Z et al (2018) Multiscale hierarchical design of a flexible piezoresistive pressure sensor with high sensitivity and wide linearity range. *Small* 14(27):1800819. <https://doi.org/10.1002/smll.201800819>
 26. Zhong W, Liu C, Liu Q et al (2018) Ultrasensitive wearable pressure sensors assembled by surface-patterned polyolefin elastomer nanofiber membrane interpenetrated with silver nanowires. *ACS Appl Mater Interfaces* 10(49):42706–42714. <https://doi.org/10.1021/acscami.8b12363>
 27. Benjamin CKT, Chortos A, Dunn RR et al (2014) Tunable flexible pressure sensors using microstructured elastomer geometries for intuitive electronics. *Adv Funct Mater* 24(34):5427–5434. <https://doi.org/10.1002/adfm.201400712>
 28. Gao Y, Lu C, Yu G et al (2019) Laser micro-structured pressure sensor with modulated sensitivity for electronic skins. *Nanotechnology* 30(32):325502. <https://doi.org/10.1088/1361-6528/ab1a86>
 29. Zhao X, Hua Q, Yu R et al (2015) Flexible, stretchable and wearable multifunctional sensor array as artificial electronic skin for static and dynamic strain mapping. *Adv Electron Mater* 1(7):1500142. <https://doi.org/10.1002/aelm.201500142>
 30. Wei Y, Chen S, Lin Y et al (2015) Cu–Ag core–shell nanowires for electronic skin with a petal molded microstructure. *J Mater Chem C* 3:9594–9602. <https://doi.org/10.1039/C5TC01723H>
 31. Yao HB, Ge J, Wang CF et al (2013) A flexible and highly pressure-sensitive graphene–polyurethane sponge based on fractured microstructure design. *Adv Mater* 25(46):6692–6698. <https://doi.org/10.1002/adma.201303041>
 32. Ge G, Cai Y, Dong Q et al (2018) A flexible pressure sensor based on rGO/polyaniline wrapped sponge with tunable sensitivity for human motion detection. *Nanoscale* 10:10033–10040. <https://doi.org/10.1039/C8NR02813C>
 33. Xu M, Gao Y, Yu G et al (2018) Flexible pressure sensor using carbon nanotube-wrapped polydimethylsiloxane microspheres for tactile sensing. *Sens Actuat A* 284:260–265. <https://doi.org/10.1016/j.sna.2018.10.040>
 34. Yu G, Hu J, Tan J et al (2018) A wearable pressure sensor based on ultra-violet/ozone microstructured carbon nanotube/polydimethylsiloxane arrays for electronic skins. *Nanotechnology* 29(11):115502. <https://doi.org/10.1088/1361-6528/aaa855>
 35. Tewari A, Gandla S, Bohm S et al (2018) Highly exfoliated MWNT–rGO ink-wrapped polyurethane foam for piezoresistive pressure sensor applications. *ACS Appl Mater Interfaces* 10(6):5185–5195. <https://doi.org/10.1021/acscami.7b15252>
 36. Pang Y, Zhang K, Yang Z et al (2018) Epidermis microstructure inspired graphene pressure sensor with random distributed spinosum for high sensitivity and large linearity. *ACS Nano* 12(3):2346–2354. <https://doi.org/10.1021/acsnano.7b07613>
 37. Bu T, Xiao T, Yang Z et al (2018) Stretchable triboelectric–photonic smart skin for tactile and gesture sensing. *Adv Mater* 30(16):1800066. <https://doi.org/10.1002/adma.201800066>
 38. Dong X, Wei Y, Chen S et al (2018) A linear and large-range pressure sensor based on a graphene/silver nanowires nanobiocomposites network and a hierarchical structural sponge. *Compos Sci Technol* 155:108–116. <https://doi.org/10.1016/j.compscitech.2017.11.028>
 39. Guo Y, Guo Z, Zhong M et al (2018) A flexible wearable pressure sensor with bioinspired microcrack and interlocking for full-range human–machine interfacing. *Small* 14(44):1803018. <https://doi.org/10.1002/smll.201803018>
 40. Peng S, Blanloeuil P, Wu S et al (2018) Rational design of ultrasensitive pressure sensors by tailoring microscopic features. *Adv Mater Interfaces* 5(18):1800403. <https://doi.org/10.1002/admi.201800403>
 41. Wu W, Wen X, Wang ZL (2013) Taxel-addressable matrix of vertical-nanowire piezotronic transistors for active and adaptive tactile imaging. *Science* 340(6135):952–957. <https://doi.org/10.1126/science.1234855>
 42. O'Rourke MF, Pauca A, Jiang XJ (2001) Pulse wave analysis. *Br J Clin Pharmacol* 51(6):507–522. <https://doi.org/10.1046/j.0306-5251.2001.01400.x>
 43. Wu Q, Qiao Y, Guo R et al (2020) Triode-mimicking graphene pressure sensor with positive resistance variation for physiology and motion monitoring. *ACS Nano* 14(8):10104–10114. <https://doi.org/10.1021/acsnano.0c03294>

Springer Nature or its licensor (e.g. a society or other partner) holds exclusive rights to this article under a publishing agreement with the author(s) or other rightsholder(s); author self-archiving of the accepted manuscript version of this article is solely governed by the terms of such publishing agreement and applicable law.